

Triplet Emitters for OLED Applications. Mechanisms of Exciton Trapping and Control of Emission Properties

Hartmut Yersin

Institut für Physikalische Chemie, Universität Regensburg, 93040 Regensburg, Germany
hartmut.yersin@chemie.uni-regensburg.de

1	Introduction	2
2	OLED Structure and Device Architecture	4
3	Exciton Formation and Energy Harvesting in the Triplet State	8
3.1	Model of Exciton Formation	8
3.2	Charge Transfer States and Relaxation Paths	11
3.3	Triplet Harvesting	12
3.4	Exciton Trapping at a Matrix Site and Energy Transfer	14
4	Ordering Scheme for Organometallic Triplet Emitters.	15
5	Photophysical Properties of Triplet Emitters Controlled by Metal Participation.	18
5.1	Singlet-Triplet Splitting	18
5.2	Inter-System Crossing	19
5.3	Phosphorescence Decay Time.	20
5.4	Zero-Field Splitting	20
5.5	Emission Band Structure and Vibrational Satellites.	21
5.6	Electronic Charge Distribution and Excited State Reorganization	22
6	Summary and Conclusion.	22
	References	23

Abstract Triplet emitter materials present attractive possibilities for optimizations of organic/organometallic light emitting diodes (OLEDs). This is due to the significantly higher efficiencies obtainable with these compounds as compared to organic emitters. In this contribution, first a schematic introduction is given, how an OLED device is built-up and why multi-layer structures are preferred. Then a basic model is presented, how electron-hole recombination, i.e. the exciton formation process, can be visualized and how the singlet and triplet states of the (doped) emitter compounds are populated. This takes place by specific singlet and triplet paths. The occurrence of such paths is explained by taking into account that the dynamical process of exciton trapping involves dopant-to-matrix charge transfer states ($^{1,3}\text{DMCT}$ states). It is also explained, why the excitation energy is harvested in the lowest triplet state of organo-transition-metal complexes. Due to spin statistics, one can in principle obtain an efficiency of a factor of four higher than using organic singlet emitter molecules. Simple comparisons suggest that electron-hole recombination should preferentially occur on the triplet emitter itself, rather than on ma-

trix molecules with subsequent energy transfer to the emitter. Further, it is pointed out that essential photophysical properties of organometallic triplet emitters depend systematically on the metal participation in the triplet state and on the effective spin-orbit coupling. These factors control the amount of zero-field splitting (ZFS) of the triplet state into substates. Increase of ZFS corresponds to higher metal character in the triplet state. Higher metal character reduces the energy difference between excited singlet and triplet states, enhances the singlet-triplet intersystem crossing rate, lowers the emission decay time, changes the vibrational satellite structure, decreases the excited state reorganization energy, etc. These effects are discussed by referring to well characterized compounds. Based on a new ordering scheme presented for triplet emitter materials, a controlled development of compounds with pre-defined photophysical properties becomes possible.

Keywords Triplet emitters · OLED · Organic/organometallic light emitting diode · Exciton trapping · Emission properties · Electroluminescence · Electrophosphorescence · Ordering scheme for triplet emitters

1

Introduction

Transition metal compounds with organic ligands or organometallic compounds¹ find an increasing interest due to their large potential for new photophysical and photochemical applications. This is particularly valid for compounds which exhibit high emission quantum yields from the lowest triplet states to the singlet ground states. Such compounds are frequently found. Their emission colors may lie in the whole visible range from the blue to the red and also in the IR. The emission decay times are usually orders of magnitude longer than those of purely organic singlet emitters. The compounds are often photo-redox active involving the triplet states and can be stable over the whole redox cycle. These photo-redox properties are important, for example, in systems that convert solar energy into electrical or chemical energy [1–3]. Moreover, emission spectra or decay times of the organometallic compounds are often sensitive to environmental factors, such as oxygen, water, rigidity of the environment, pH value, specific organic vapors, concentration of glucose, or simply vary with temperature, etc. Thus, these compounds are also in the focus of the strongly developing field of luminescence sensors [4–10].

In the scope of this chapter, organometallic triplet emitters are of particular interest due to their promising use in electro-luminescent devices such as OLEDs (organic/organometallic light emitting diodes). (See for example [11–16].) In Sect. 2, the construction and working principle of an OLED is

¹ In the chemical nomenclature *organometallic compounds* contain direct metal-carbon bonds, while this is not necessarily the case for *metal compounds with organic ligands*. In the scope of this review, however, this distinction is not always important. Therefore, mostly the shorter term organometallic compounds is used in a more general meaning.

presented on an introductory basis. Specifically, by use of organometallic compounds, it is possible to obtain, at least in principle, a four times higher electro-luminescence efficiency than with typical singlet emitters. This property is related to the specific mechanisms of exciton formation in the electron-hole recombination zone and to fast and efficient intersystem crossing (ISC) from the excited singlet to the light emitting triplet state. This process of accumulating the excitation energy in the lowest excited triplet state is often called *triplet harvesting*. These mechanisms are addressed in detail in Sect. 3.

The triplet states of the emitter materials play an essential role in OLEDs. Therefore, it is highly desirable to control the properties of these states and to synthesize compounds with pre-defined behavior. However, this is only achievable if a good understanding of the electronic structures of the states involved in the emission process is available. In particular, it is very useful to know how these electronic states react on chemical variations, changes of the environment or temperature. Obviously, there are already important approaches to these objectives available. For example, variations of emission energies and redox-potentials with ligand replacements or substitutions have been studied especially for complexes of Ru(II) and Os(II) [17–22], but also of Re(I) [23, 24], Ir(III) [13, 25] and others (e.g., see [12, 22, 26–29])². Modifications of emission properties with solvent or matrix variation have been described for many organometallic compounds [22, 23, 30–34]. Of particular interest are those factors that determine emission decay times and photoluminescence quantum yields. In this respect, one has to consider symmetry effects, spin-orbit coupling (SOC) of the emitting state to higher lying states, self-quenching (for example, by triplet-triplet annihilation resulting from interactions between adjacent excited emitter compounds), radiationless energy transfer to impurity centers, vibronic coupling, vibrational energies, coupling to the environment, etc. Specifically, vibronic coupling is responsible for radiationless deactivation. This coupling leads to the well-known energy gap law. It relates the increase of radiationless deactivation and thus a decrease of photo-luminescence quantum yield and emission decay time to a decrease of the energy separation between the emitting state and the ground state (see for example [20, 23, 30, 32, 35]; for background information see also [35–39]).

In the present investigation, a different strategy leading to a control of photophysical properties is discussed. In this approach, a new ordering scheme is presented which is based on the extent of metal participation, such as 4d or 5d orbital character, in the emitting triplet state. The metal participation in the corresponding wavefunction is also responsible for the importance of spin-orbit coupling. Interestingly, the corresponding extent of these influences is displayed in the size of the splitting of the triplet state

² References are only given as examples.

into substates, the total zero-field splitting (ZFS). This parameter can be varied over more than three orders of magnitude by appropriate combination of the transition metal ion and the organic ligands. This ordering scheme is presented in Sect. 4. The essential photophysical effects that are induced by the increasing metal character in the triplet state are discussed in Sect. 5. The paper is concluded with Sect. 6.

2 OLED Structure and Device Architecture

Figure 1 shows the basic and simplified structure of an OLED which is largely built up of organic materials. Under action of a driving voltage of 5 to 10 V or even lower, electrons are injected from a metal cathode with a low work function into the electronic state corresponding to the LUMO (lowest unoccupied molecular orbital) of the adjacent layer material (electron transporting layer). In this layer, the electrons hop via the LUMOs of neighboring molecules towards the anode. The hopping process under action of an exter-

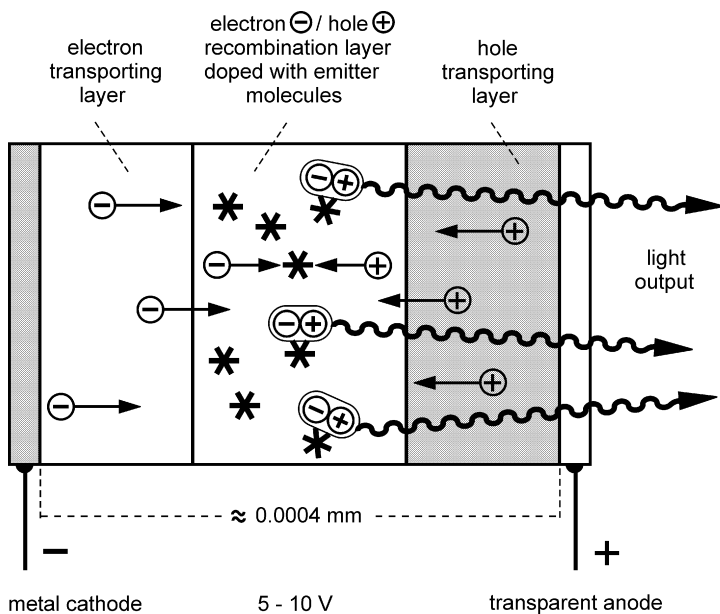


Fig. 1 Basic set-up of a layered OLED structure. Electrons and holes are injected from the respective electrodes (metal cathode, semiconducting and transparent anode). The charge carriers move from different sides into the recombination/emitter layer, where electrons and holes recombine and excite the doped emitter molecules (asterisks, e.g., organometallic triplet emitters). For more details see Fig. 2. For clarity, light emission is only shown for one direction although the photons are emitted in all directions

nal driving potential is related to a specific electron mobility. It is remarked that the electron mobility in organic materials is orders of magnitude smaller than in crystalline inorganic semiconductors. This is due to the quasi-localized nature of the electronic states in disordered (amorphous) organic materials, the relatively small overlap of electronic wavefunctions of neighboring molecules, and other irregularities of molecular packing within the layers. The charge carrier transport occurs in these disordered materials mainly by thermally activated hopping processes.

The anode of the device is a transparent semiconducting layer which usually consists of a nonstoichiometric composite of SnO_2 (10–20%) and In_2O_3 (90–80%), usually called indium tin oxide (ITO). This material is coated, for example, on a glass support. The ITO layer exhibits a low work function for hole³ injection into the highest occupied molecular orbital (HOMO) of the organic material which acts as hole conducting layer. Again, the hole mobility in the amorphous organic layer material is much smaller than the mobility via the valence band of an inorganic semiconductor.

Both particles, electron and hole—coming from the different electrodes—move from opposite directions towards the recombination layer. There they can combine and form excitons. This may happen near to the layer interface, on matrix molecules within the layer, and/or at doped emitter molecules. In suitable cases, as required for OLEDs, this leads to a population of excited states of the emitter material which subsequently emits light. Obviously, this process should occur with high efficiency. Details of the mechanism of exciton formation and population processes of excited emitter states are discussed in the next section.

The simple set-up of an OLED as presented in Fig. 1 is in most cases not well suited to exploit the potential of efficiency of light emission that is in principle obtainable. Independent from the quantum efficiency of the emitter molecules, losses can occur for several reasons, such as poor adjustments of workfunctions of the electrodes relative to the HOMO/LUMO of the adjacent organic layers, bad alignments of HOMOs and LUMOs of the different organic layers relative to each other which can cause charge carrier trapping and unfavorable space charges, unbalanced electron and hole transports, low electron or hole mobility which can lead to ohmic losses, low cross sections for electron-hole recombination, low light outcoupling efficiency, etc.

³ The HOMO of a neutral organic molecule is usually populated with two electrons. If one electron is taken off, for example by transferring it to the anode, the remaining situation is characterized by a positively charged molecule. Subsequently, the free electron position in the HOMO can be populated by an electron from the HOMO of a neighboring molecule. Thus, the positive charge has moved to the neighbor. An equivalent process occurs involving the next nearest neighbor, and so on. Thus, the positive charge—called a hole—moves from molecule to molecule into direction of the cathode. Such a hole has properties of a particle, it carries a positive charge, a spin (the one of the residual electron) and can move with a specific hole mobility by use of the HOMOs.

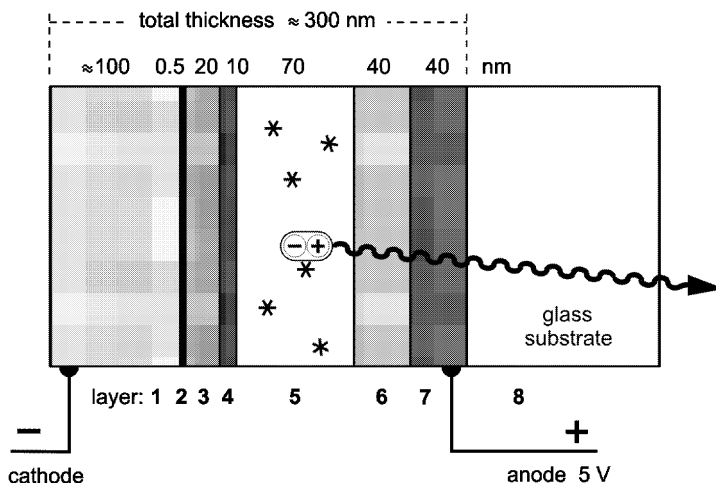


Fig. 2 Example of an optimized OLED structure. (1) (2): cathode, Ag and LiF. (3): electron transporting layer; Alq₃ (=Alqol₃). (4): hole blocking layer, BCP. (5): electron-hole recombination zone/emitter layer, PVK doped, for example, with Ir(ppy)₃. (6) and (7): anode, PEDOT doped with PSS (6) for improvement of hole injection and substrate smoothness and ITO (7) (=indium tin oxide). (8): glass support. For further details and explanations see text

The OLED technology is far from being completely developed, although substantial progress has been made during the last years.

An improved OLED device structure is displayed in Fig. 2 and will subsequently be discussed on an introductory basis. By careful adjustment of the different layers a much more efficient OLED can be constructed (device architecture). The device shown consists of eight layers including the electrodes and the glass support. (1) and (2): The cathode is mostly built-up by a bi-layered material to reduce the work function of electron injection. For example, Al/LiF [40, 41] or Ag/MgAg [42, 43] are frequently applied. (3): In most devices, Alq₃ (q⁻=qol⁻=8-quinolinolato-O,N) is used as electron transporting layer [40–45]. (4): Holes, coming from the anode, have to be present with high density in the recombination layer, but they should be blocked from further transport to the cathode. Therefore, hole blocking increases the efficiency of light emission. This is achieved by a material with a sufficiently low lying HOMO (e.g., see [44]). On the other hand, it is important that this layer does not block electron transport. In many cases, BCP (bathocuproine=4,7-diphenyl-2,9-dimethyl-1,10-phenanthroline) has been employed as hole blocking layer [16, 40, 42–44]. (5): In the recombination or emitter layer, holes and electrons have to be accumulated at high, but balanced densities and should recombine to induce light emission. The device efficiency depends essentially on the emitter compound as well as on the

matrix material of layer (5). Particularly efficient emitter compounds are organo-transition-metal complexes, which are in the focus of this contribution. They are doped into a suitably selected layer (matrix) material. It seems to be advantageous, when the electron-hole recombination occurs directly at the doped emitter molecules (see Sects. 3.1 and 3.4). Obviously, the HOMO and LUMO positions of the emitter layer matrix material have to fit to those of the adjacent layers as well as to the oxidation potential of the electronic ground state and to the reduction potential of the (active) excited state of the doped emitter. Moreover, the triplets of the matrix molecules have to lie at higher energies than the triplets of the doped emitter molecules. Otherwise, the emission of the dopants would be quenched. A successful emitter layer is, for example [43], PVK (polyvinylcarbazole) doped with about 5 wt% Ir(ppy)₃ (fac-tris(2-phenylpyridine)Ir(III)). PVK represents a good hole transporting polymer. It is remarked that also several other matrix materials have successfully been tested with Ir(ppy)₃ as emitter compound (e.g., see [40, 44]). However, in this latter case other materials of the adjacent layers might be required to obtain a fit of the potentials. (6) and (7) are the anode layers. (7) is the transparent ITO anode, while (6) is a material used to improve hole injection and substrate smoothness. For this material PEDOT (poly(ethylenedioxythiophene) doped with polystyrenesulfonic acid (PSS) has, for example, been applied [43, 46]. It is remarked that good contact between the ITO and the PEDOT:PSS layers is crucial. Thus, specific cleaning of the ITO substrate, for example, by oxygen plasma or UV ozone treatment is required, e.g. see [47, 48]. (8): Finally, the layers discussed so far have to be positioned on a support, since the total thickness of the layers (1) to (7) is only about 300 nm (Fig. 2). Mostly, a glass support is employed.

Obviously, the state of art of research and development of highly efficient devices cannot be summarized in this introductory discussion of device architecture. This would be outside the scope of the present review. Here it is only possible to point to several recent further developments in various fields, such as (i) improvement of light outcoupling by controlling interference effects [49, 50], (ii) increase of charge carrier mobilities by doping of donors into electron conducting materials or acceptors into hole-transporting layers [51], (iii) improvement of adaption of workfunctions for hole and electron injection and optimization of redox potentials of the different layers (compare review [45]), (iv) development of materials with sufficiently high glass-transition temperature to avoid crystallization [45], (v) use of organosiloles as electron transporting materials [52–55], (vi) high-efficiency white light OLEDs [56], (vii) techniques for increase of device lifetime by device encapsulation to prevent water or oxygen penetration [57, 58], and (viii) materials and/or methods for better or less expensive OLED fabrication [59–61], etc.

3 Exciton Formation and Energy Harvesting in the Triplet State

3.1 Model of Exciton Formation

It is instructive to discuss how the process of electron-hole recombination and the formation of a neutral exciton and finally the population of an excited state of the emitter molecule can be visualized. Here, we focus on processes that occur within the emitter layer (layer (5) in Fig. 2). This layer of a thickness of about 70 nm consists of an organic matrix which is doped with emitter molecules (dopants). In the subsequent model it is assumed that the recombination of electrons and holes occurs at the dopants. The importance of this process has been deduced by comparison of photoluminescence and electroluminescence properties [62, 63]. If the matrix is excited optically, one observes an emission of both matrix and dopant. The intensity of the latter one increases gradually with the concentration of the dopant. Its emission can be ascribed to result from a radiationless energy transfer from the initially photo-excited matrix to the dopant. Thus, relatively high dopant concentrations are required to achieve quenching of matrix emission. On the other hand by electro-luminescent excitation, the concentration of the dopant can be reduced by more than two orders of magnitude to achieve complete quenching of matrix emission. Only dopant emission is observable. These results [62, 63] show that one of the charge carriers, either hole or electron, is trapped first at the dopant. For completeness, it is remarked that the effective recombination zone can be significantly thinner than the whole emitter layer, since the recombination may occur near to a layer interface within a range of only 5–10 nm due to a high density of charge carriers in this region [16, 64]. In Sect. 3.4 the processes of exciton formation and trapping are addressed again to focus on an aspect of OLED material design.

Figure 3 displays a simplified and schematic model to describe the process of exciton formation. The first step is characterized by trapping of a charge carrier. In our model it is assumed that the hole is trapped first at the emitter molecule as proposed, for example, for $\text{Ir}(\text{F-ppy})_3^4$ in PVK [65]. This process induces (for a short time interval) the formation of an oxidized $\text{Ir}(\text{F-ppy})_3$ complex. However, trapping of an electron as first step would result in an equivalent model and might be of relevance for other emitter molecules. For example, a corresponding process might be demanded for emitter layers doped with compounds which exhibit irreversible oxidation, as found for several Pt(II) complexes [12]. The process of charge carrier trapping can induce a reorganization at the emitter molecule which means that intramolecular distances, electronic energies, interactions with the environ-

⁴ fac-tris[2-(4',5'-difluorophenyl)pyridine]Ir(III)

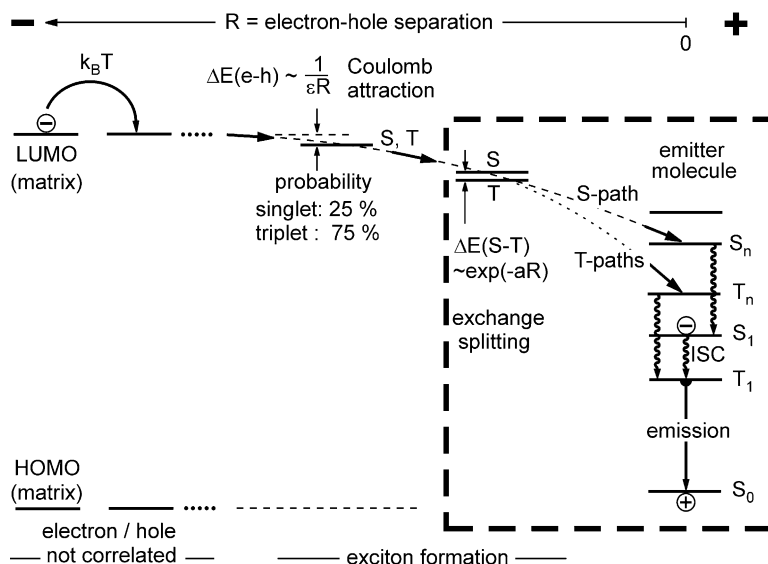


Fig. 3 Dynamics of exciton formation. It is assumed that the hole (+) is trapped first on the doped emitter molecule. The exciton formation starts due to Coulomb interaction between the trapped hole and the electron (-) on a matrix molecule. At the beginning of the exciton formation the spins of hole and electron are already correlated to one singlet and three triplet substates. This corresponds in a statistical limit to a ratio of 25% to 75%. The S-path and T-path populate the excited states of the emitter molecule (exciton trapping process). These paths can also be interpreted as relaxation processes from dopant-to-matrix charge transfer states. The DMCT states are deduced from the situation displayed in the framed part shown at the right hand side of the figure. The corresponding energy level diagram is depicted in Fig. 4. For clarity, the diagram does not show shifts of matrix orbitals due to the external potential, also reorganization energies are not depicted in the figure. ISC: intersystem crossing, ΔE (e-h): electron (e)-hole (h) binding energy; ΔE (S-T): singlet-triplet splitting

ment, etc. can be altered. The corresponding effects depend strongly on the individual emitter molecule and its specific matrix environment. They are not depicted in the model of Fig. 3. Under an applied external potential, the electron will migrate along the matrix material towards the anode. Usually, this process of electron hopping (more exactly: polaron hopping⁵) requires a thermal activation energy due to inhomogeneities from spatial and energy disorder and due to matrix reorganization effects. The related energy shifts should be less or of the order of the thermal energy $k_B T$ with k_B being the Boltzmann constant and T the absolute temperature. For clearness, the dia-

⁵ Electron (or hole) hopping is normally connected with a polarization of the matrix. Therefore, the corresponding negatively (positively) charged particle represents a polaron (for background information see, for example, [66]).

gram is simplified and does not show the inhomogeneous distribution of the energy levels of the matrix molecules and their energy shifts induced by the external potential.

When the electron is still far from the trapped hole, it will migrate independently from this hole towards the anode. Thus, hole and electron are not bound or correlated. This situation corresponds to the exciton continuum in solid-state semiconductors (see left hand side of the diagram, Fig. 3). However, when the electron migrates into a region given by a specific electron-hole separation R , the positively charged hole will attract the electron. This separation is reached when the energy of the Coulomb attraction is of similar size as the larger one of the two values, the mean inhomogeneous distribution of the energy levels of the matrix material or the thermal energy $k_B T$. Due to the Coulomb attraction, an electron (e)-hole (h) binding results. The binding energy $\Delta E(e-h)$ depends on the separation R and on the electric permittivity (dielectric constant ϵ) of the matrix material. Induced by this attraction, the exciton is formed. The Coulomb attraction represents a long-range interaction as compared to nearest neighbor separations.

For the further processes, it is required to take also the spins of both electron and hole into account. The spin of the hole is given by the spin of the residual electron at the emitter molecule. In a quantum mechanical treatment, these spins can be coupled to *four* new combined states. One obtains *one* singlet state and one triplet state. The triplet consists of *three* triplet substates. These substates differ from each other mainly by their relative spin orientations. An energy splitting between the resulting singlet and triplet states may be disregarded at large electron-hole separations. Therefore, the corresponding exciton state is shown in Fig. 3 (middle) just by one energy level. In a statistical limit, all *four* substates of this exciton state will be formed (populated) with an equal probability. Consequently, one obtains a *population ratio of one to three* for singlet and triplet substates, respectively.

Driven by electron-hole attraction, the electron will further move on matrix molecules towards the trapped hole. At least, when the electron reaches nearest neighbor matrix molecules of the emitter, an overlap of electron and hole wavefunctions has also to be taken into account. The resulting (short-range) exchange interaction leads to an energy splitting of singlet (S) and triplet (T) states by $\Delta E(S-T)$. As depicted in Fig. 3, this energy depends approximately exponentially on the electron-hole separation (a is a constant which depends on the respective matrix and the emitter material).

In a final step, the electron jumps in a very fast process directly to the emitter molecule and it results an excited emitter. This process may occur as singlet or triplet path (S-path, T-path) depending on the initial spin orientation of the electron-hole pair. The corresponding time constants are of the order of one picosecond (see next section). The population of S_n and T_n states, as shown in Fig. 3, is only depicted as an example. Subsequently, the system will exhibit the usual behavior of an optically excited emitter mole-

cule with typical relaxation processes to the lowest excited states and typical emission properties (right hand side of Fig. 3).

3.2

Charge Transfer States and Relaxation Paths

The final steps of the mechanisms described above can also be discussed in a slightly different way, to illustrate the occurrence of specific singlet and triplet paths. The situation of a lacking electron in the ground state of the doped emitter molecule (dopant D) and of additional electron charge density on nearest neighbor matrix molecules M can be characterized by dopant-

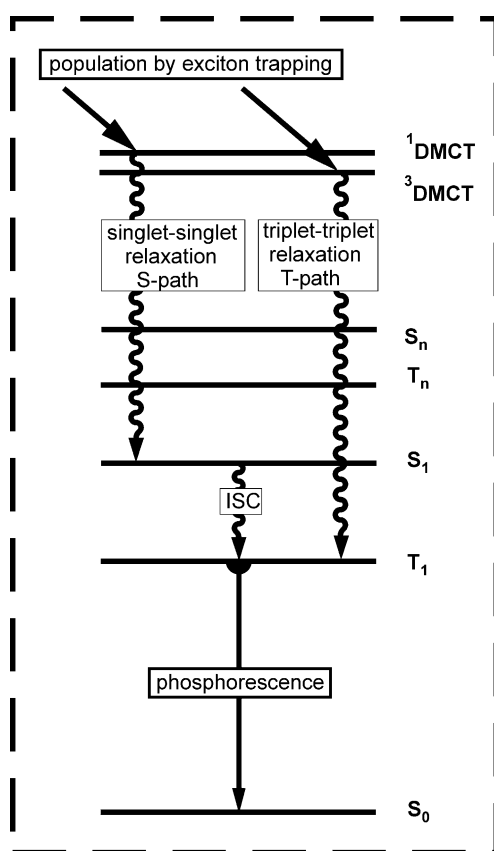


Fig. 4 Energy level diagram of an emitter compound with its first coordination sphere of matrix molecules. The states $^1\text{DMCT}$ and $^3\text{DMCT}$ represent dopant-to-matrix charge transfer states. The lower lying states are largely those of the isolated emitter molecule itself. The relaxations from the $^1\text{DMCT}$ and $^3\text{DMCT}$ states, respectively, represent the S-path and T-path of exciton formation as depicted in Fig. 3

to-matrix charge transfer (DMCT) states, specifically by singlet ($^1\text{DMCT}$) and triplet ($^3\text{DMCT}$) states.

It may be visualized that these states belong to a large molecular complex that consists of the doped emitter itself and of the first nearest neighbor sphere of matrix molecules. The energy level diagram of this emitter-matrix-cage unit is schematically displayed in Fig. 4. It corresponds to the framed part of Fig. 3. In particular, the states S and T shown in the frame represent the $^1\text{DMCT}$ and $^3\text{DMCT}$ states of the large molecular unit. The lower excited states S_0 , T_1 , S_1 to S_n are largely confined to the doped molecule itself, while the higher lying charge transfer states are spatially more extended to the first matrix coordination sphere. For these latter states, the exchange interaction between the two electrons involved is relatively small. Thus, the energy separation between the $^1\text{DMCT}$ state and the $^3\text{DMCT}$ state is expected to be much smaller than singlet-triplet separations of the spatially more confined states of the original dopant itself.

On the basis of the energy level diagram of Fig. 4, one also obtains information about the relaxation paths from the excited charge transfer states. In particular, the relaxation from the $^1\text{DMCT}$ to lower states will be faster within the system of singlet states than making a spin-flip first. This is due to the fact that spin-orbit coupling in the organic matrix material will be relatively small and, thus, intersystem crossing (ISC) is not favored. Consequently, one obtains the fast singlet path that finally populates the S_1 state. (Figs. 3 and 4). Subsequently, the population of the S_1 state will be followed by an ISC to the T_1 state, though usually with a smaller rate (see also next subsection). An initial population of the $^3\text{DMCT}$ state is similarly followed by a very fast relaxation within the system of triplet states down to the lowest triplet state T_1 (Fig. 4). The beginning of this relaxation process corresponds to the triplet path in the exciton trapping model shown in Fig. 3. The relaxation times within the singlet and triplet system, respectively, are of the order of one picosecond or faster, while the ISC processes can be significantly slower (see next section).

In conclusion, it is remarked that the exciton trapping process and thus the efficiency of light emission in an OLED will usually depend on both the emitter molecule and the matrix environment.

3.3 Triplet Harvesting

Spin-orbit coupling will not strongly alter the mechanism of exciton formation in an organic matrix material, but it will have drastic effects on the efficiency of electro-luminescence in an OLED device. To illustrate this property, we will compare the efficiency which is obtainable with a purely organic molecule to the efficiency achievable with a transition metal complex, if both molecules exhibit equal photo-luminescence quantum yields. If one as-

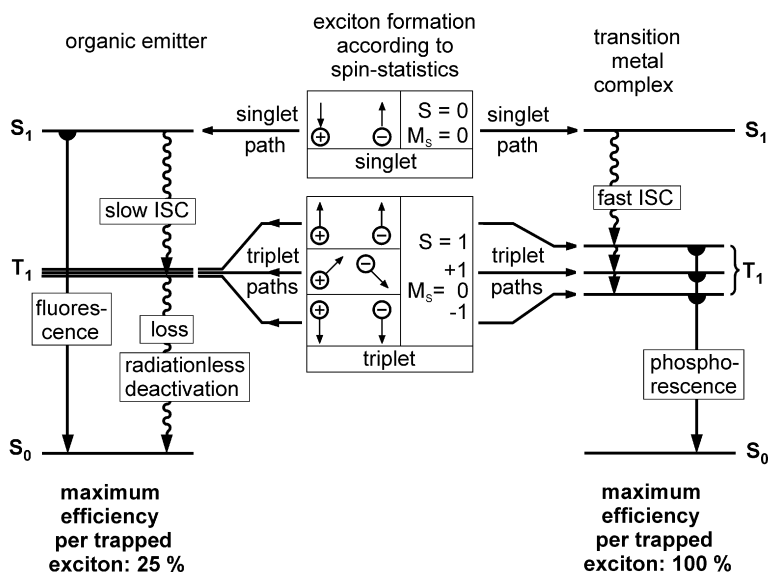


Fig. 5 The diagram explains the effect of triplet harvesting. Due to spin-statistics, electron-hole recombination leads to 25% singlet and 75% triplet state population. In organic molecules, only the singlets emit light (fluorescence), while the triplet excitation energy is transferred into heat (left hand side). On the other hand, organometallic compounds with transition metal centers do not exhibit a fluorescence, but show a fast intersystem crossing (ISC) to the lowest triplet state. Thus, the triplet *harvests* singlet and triplet excitation energy and can efficiently emit. In principle, a triplet emitter can—in the limit of vanishing radiationless deactivations—exhibit a four times higher electroluminescence efficiency than a singlet emitter

sumes that the initial process of exciton formation occurs statistically with respect to the spin orientations, one obtains 25% of excitons with singlet character and 75% with triplet character. At least for small molecules, this view is largely accepted⁶.

After exciton formation and relaxations according to the specific singlet and triplet paths, as discussed in the preceding section, the lowest excited singlet and triplet states are populated. This is valid for organic as well as for organo-transition-metal emitter materials. The corresponding processes are schematically displayed in the middle of Fig. 5. The organic molecule can exhibit an efficient emission as $S_1 \rightarrow S_0$ fluorescence, since usually the $S_1 \rightarrow T_1$ intersystem crossing rate is small. On the other hand, since the radiative $T_1 \rightarrow S_0$ rate is also small, the deactivation of the T_1 state occurs normally non-radiatively at ambient temperature. Therefore, 75% of the excitons, the

⁶ Currently it is discussed in the literature that for large conjugated polymers spin-statistics might not be applicable; however, this discussion is irrelevant for triplet emitters with high ISC rates (compare [67–74]).

triplet excitons, are lost. Their energy is transferred into heat (Fig. 5, left hand side). The conditions are more favorable for transition metal complexes, in which the central metal ion carries significant spin-orbit coupling (Fig. 5, right hand side). This is particularly valid for metal ions of the second and third row of transition metals. For these complexes, ISC to the lowest T_1 state is usually very efficient and thus a singlet S_1 emission is not observable. Moreover, the radiative $T_1 \rightarrow S_0$ rate can become sufficiently high so that efficient phosphorescence can occur, even at ambient temperature (for a more detailed discussion see below). Consequently, all four possible spin orientations of the excitons can be harvested to populate the lowest T_1 state. In conclusion, by this process of *triplet harvesting* one can in principle obtain a four times larger electro-luminescence efficiency for triplet emitters than for singlet emitters. This factor of four can be attained if the radiationless deactivation is equal for both emitter types.

3.4

Exciton Trapping at a Matrix Site and Energy Transfer

Exciton formation and trapping can also occur at matrix sites. Both the lowest singlet and triplet states of matrix molecules will be populated. From there, triplet and singlet exciton diffusion as Frenkel excitons can occur, although with different transport probabilities. This will alter the spatial distribution of matrix molecules that are excited in singlet and triplet states, respectively, as compared to the situation immediately after excitation. For an efficient OLED, it is mostly required to harvest the excitation energy completely in an efficiently phosphorescent triplet state of an organometallic dopant. This requires the realization of two distinctly different, but effective processes of energy transfer (Fig. 6). For example, the singlet excitation energy is transferred by a long-range Förster transfer mechanism from a matrix molecule to the acceptor (dopant). Independently, the triplet excitation energy is transferred by a second process of energy transfer from the matrix molecule, for example, by a short-range Dexter transfer mechanism. Both transfer mechanisms should be highly efficient and therefore they should fulfill the resonance conditions. This can be expressed by non-vanishing spectral overlap integrals of donor emissions and acceptor absorptions (for background information see, for example [38]). The fulfillment of these two independent conditions for singlet and triplet energy transfer seems to make this concept of material design—apart from specific and selected combinations—less favorable, as compared to systems with charge carrier trapping directly on the triplet emitters, as discussed in Sect. 3.1 (compare also [73, 74]).

Independent from the discussion presented above, Fig. 6 also shows that the lowest triplet state of the emitter compound always has to lie at lower energy than the triplet of the matrix material. Otherwise the matrix would

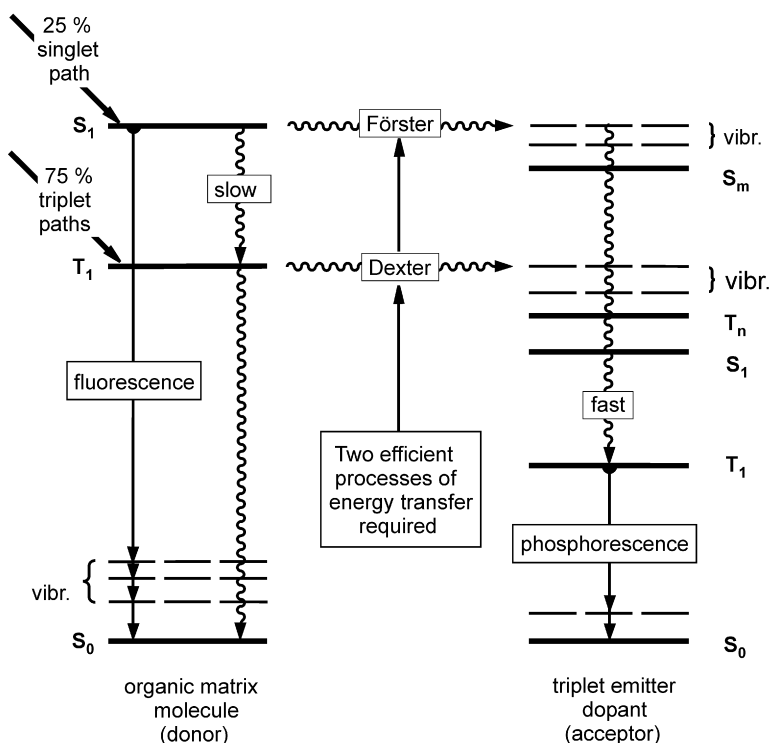


Fig. 6 Exciton trapping on organic matrix molecules with subsequent energy transfer. Exploitation of matrix singlet and triplet excitation energy requires the effectiveness of two independent processes of energy transfer. Such a matching of molecular energies might be difficult to achieve, when OLED emitter layers are developed. vibr.: vibrational states

quench the excited emitter. In a slightly different approach, one can also express the following requirement. The states corresponding to HOMO and LUMO of the dopant have to be within the gap of the states that stem from the matrix material. Thus, hole or electron trapping as the initial process is possible and quenching of emitter triplets by matrix triplets is prevented.

4 Ordering Scheme for Organometallic Triplet Emitters

Many photophysical properties of the lowest excited triplet states and the corresponding transitions of organometallic compounds are essentially determined by the extent of metal participation in the wavefunctions. This metal participation not only alters the spatial extension of the wavefunc-

tions, but also induces significant mixtures of singlet and triplet states by spin-orbit coupling (SOC) which is mainly carried by the metal orbitals. It is of interest to develop an understanding how these effects influence the photophysical properties of emitter materials. Indeed, this is possible. Moreover, it can be shown that a simple ordering scheme can be helpful in this respect [75–79]. Specifically, the energy splitting of the triplet state into sub-states, the zero-field splitting (ZFS) measured in cm^{-1} , can be utilized, since this parameter displays the importance of metal character and SOC for the respective triplet state.

The amount of ZFS is usually determined spectroscopically. Nevertheless, it is instructive to visualize that it is dominantly controlled by specific interactions. For example, the splitting of a pure $^3\pi\pi^*$ state which is not metal-perturbed is only given by spin-spin interactions (e.g., see [38, 80–82]). In this situation, the ZFS is of the order of 0.1 cm^{-1} . However, if $^3\text{MLCT}$ and $^1\text{MLCT}$ states are in proximity, the substates of these latter states will interact due to SOC with the substates of the $^3\pi\pi^*$ term. This can lead to a significant triplet splitting in particular, when 5d orbitals are involved in the $^1,^3\text{MLCT}$ states. As a consequence, the ZFS can increase by more than three orders of magnitude, up to more than 200 cm^{-1} [75–79]. The amount of ZFS can be determined, at least formally, by second order perturbation theory, whereby the perturbation is given by the spin-orbit Hamiltonian. The resulting matrix elements that induce the coupling are essentially controlled by d-orbital participation in the admixing wavefunction (compare also [81–86]).

Figure 7 shows a sequence of a series of compounds which are arranged according to an increasing ZFS of the emissive triplet state. The ZFS values of most of the compounds have been determined from highly resolved optical spectra [34, 75–79] (references for the individual compounds are given in [79]). Only for $\text{Ir}(\text{ppy})_3$ [87] and $\text{Ir}(\text{ppy})_2(\text{CO})(\text{Cl})$ [25] were such resolved spectra not yet obtainable, and therefore the information was determined indirectly from the temperature dependence of the emission decay time.

The low-lying electronic states of the compounds shown in Fig. 7 have to be assigned to different types of frontier orbital transitions. Thus, the lowest triplets of $[\text{Rh}(\text{bpy})_3]^{3+}$ and $[\text{Pt}(\text{bpy})_2]^{2+}$ are characterized as ligand centered $^3\text{LC}(^3\pi\pi^*)$ states with very small metal admixtures and those of $[\text{Ru}(\text{bpy})_3]^{2+}$, $\text{Ir}(\text{ppy})_3$, $[\text{Os}(\text{bpy})_3]^{2+}$, and $[\text{Os}(\text{phen})_3]^{2+}$ represent $^3\text{MLCT}$ (metal-to-ligand charge transfer) states. The cyclometalated Pt(II)-compounds and $[\text{Pt}(\text{mnt})_2]^{2-}$ have to be assigned to intermediate situations with significant $^3\text{LC}/^3\text{MLCT}$ mixtures, whereas the lowest states of the oxinate complexes, such as $\text{Pd}(\text{qol})_2$, $\text{Pt}(\text{qol})_2$, and $\text{Pt}(\text{qtl})_2$, are characterized as $^3\text{ILCT}$ states (intra-ligand charge transfer from the phenolic moiety to the pyridine part of the ligand) with relatively small metal-d or MLCT admixtures. Nevertheless, the ordering expressed by the sequence shown in

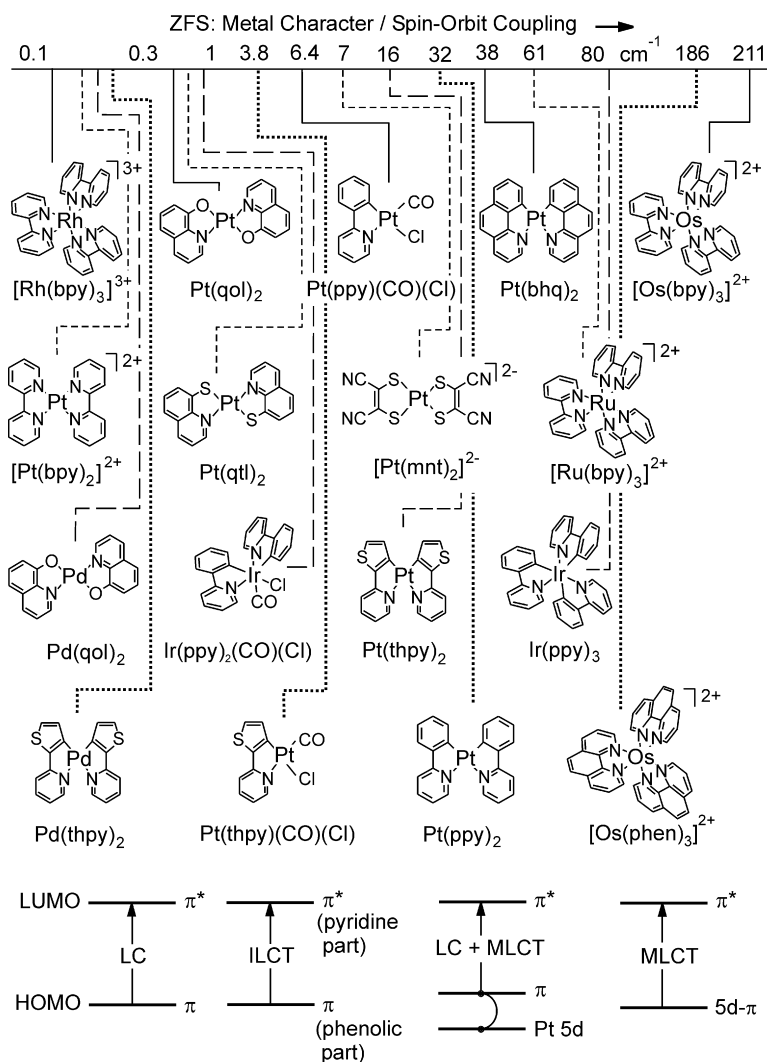


Fig. 7 Ordering scheme for organometallic triplet emitters according to the amount of zero-field splitting (ZFS) of the emissive triplet state. This splitting reflects the size of metal participation (MLCT and/or d-orbital character) and spin-orbit coupling in the corresponding wavefunctions. The diagrams *at the bottom* show energy levels of the relevant frontier molecular orbitals for the different compounds. For details see text. (Compare [79] and for the Ir(III) compounds [25, 87, 88])

Fig. 7 can in fact be employed in the sense of a controlled variation of metal participation/spin-orbit coupling. In the next section, it will be discussed how photophysical properties vary with the increase of the zero-field splitting parameter.

5 Photophysical Properties of Triplet Emitters Controlled by Metal Participation

The energy splitting (ZFS) of a triplet state into substates displays the importance of metal character and spin-orbit coupling for this state. The ZFS value varies by more than a factor of 2000 (Fig. 7). Thus, essential changes of photophysical properties are expected to occur. Several important trends will be discussed in the following subsections. This is carried out on a qualitative and introductory basis (Fig. 8). For comparison, properties of typical organic molecules ($\pi\pi^*$ emitters) are also referred to.

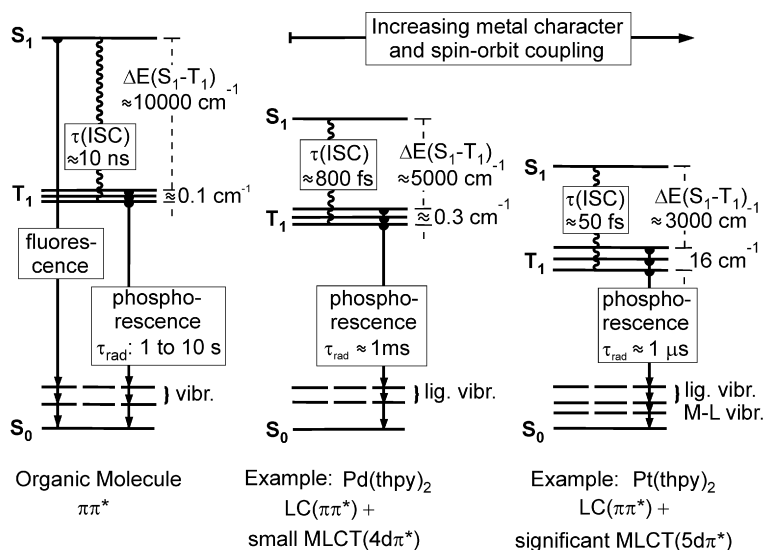


Fig. 8 Photophysical properties of a representative organic molecule compared to two organo-transition-metal emitters. The emissive triplets of Pd(thpy)₂ and Pt(thpy)₂ exhibit small and significant MLCT admixtures to the LC($\pi\pi^*$) states, respectively. The positions of the compounds in the ordering scheme and the molecular structures are found in Fig. 7. Photophysical properties of Pd(thpy)₂ and Pt(thpy)₂ are discussed in detail in [79]. lig. vibr.=ligand vibrations, M-L vibr.=metal-ligand vibration

5.1 Singlet-Triplet Splitting

Organic molecules exhibit S_1 - T_1 splittings being typically of the order of 10^4 cm^{-1} (Fig. 8) for states which stem from a $\pi\pi^*$ configuration and for molecules of similar sizes like those shown as ligands in Fig. 7. The $\Delta E(S_1-T_1)$ splitting is essentially given by the exchange interaction and is a

consequence of electron-electron interaction. For an organo-metallic compound, such as $\text{Pd}(\text{thpy})_2$, one finds a value of 5418 cm^{-1} [79]. The emissive triplet of this compound has been classified experimentally [79, 89–91] and later also by CASPT2 ab initio calculations [92] as being mainly of $\text{LC}(\pi\pi^*)$ character with a small $\text{MLCT}(4d\pi^*)$ admixture. Therefore, the compound is found at the left hand side of the ordering scheme of Fig. 7 [79]. On the other hand, for $\text{Pt}(\text{thpy})_2$ with a significant $\text{MLCT}(5d\pi^*)$ admixture to the $\text{LC}(\pi\pi^*)$ state [34, 78, 79], the amount of $\Delta E(S_1-T_1)$ is reduced to 3278 cm^{-1} [79] (Fig. 8). Obviously, enhancing of metal character in the corresponding wavefunctions increasingly reduces the $\Delta E(S_1-T_1)$ value. Due to the higher metal character, the electronic wavefunctions extend over a larger spatial region of the complex. This is connected to an on average larger spatial separation between the interacting electrons. Thus, electron-electron interaction and also exchange interaction are reduced. This explains both the lowering of the S_1 state and the reduction of $\Delta E(S_1-T_1)$ for compounds with higher metal character.

5.2

Inter-System Crossing

After excitation of the singlet state S_1 either optically or by electron-hole recombination, the organic molecule can exhibit an efficient fluorescence ($S_1 \rightarrow S_0$ emission) with a time constant of the order of 1 ns. In competition to this process, ISC can at least principally depopulate the S_1 state. However, the time constant of $\tau(\text{ISC})$ is often much larger (order of 10 ns) than the radiative decay constant of the S_1 state and thus ISC does not effectively quench the fluorescence (Fig. 8). On the other hand, in transition metal complexes, the ISC time is drastically reduced due to singlet-triplet mixing induced by SOC and due to the reduction of the energy separation $\Delta E(S_1-T_1)$. Further, due to this latter effect, the number of vibrational quanta which are responsible for the deactivation is reduced and thus the ISC process becomes even more probable. For example, already for a compound, such as $\text{Pd}(\text{thpy})_2$, with a relatively small metal participation in the wavefunction of the T_1 state and a halved $\Delta E(S_1-T_1)$ value, ISC is by four to five orders of magnitude faster (800 ps [79]) than in usual organic compounds with $^1\pi\pi^*$ and $^3\pi\pi^*$ states. For $\text{Pt}(\text{thpy})_2$ with a higher metal participation, the process is again much faster ($\tau(\text{ISC}) \approx 50 \text{ fs}$ [79]) (Fig. 8).

In conclusion, the process of inter-system crossing in organometallic compounds with transition metal ions is fast and efficient for all compounds shown in Fig. 7. The quantum efficiency for this process is often nearly one (e.g., see [4]). Therefore, an emission from the S_1 state is not observable. This property is the basis of the triplet harvesting effect discussed above.

5.3 Phosphorescence Decay Time

In pure organic molecules, the $S_0(\pi^2) \leftrightarrow T_1(\pi\pi^*)$ transition is usually strongly forbidden. The radiative decay time can be of the order of 10 s. [38] On the other hand, non-radiative processes are mostly much faster. Thus, phosphorescence from the T_1 state is normally totally quenched at ambient temperature. With increasing SOC, the radiative decay time of the $T_1 \rightarrow S_0$ transition is reduced and thus the radiative path can compete with the non-radiative one. Interestingly, already a relatively small ${}^3\text{MLCT}/{}^1\text{MLCT}$ admixture to the ${}^3\text{LC}(\pi\pi^*)$ state increases the $S_0 \leftrightarrow T_1$ transition probability drastically. For example, for $\text{Pd}(\text{thpy})_2$ the radiative decay time is reduced to be of the order of 1 ms. For $\text{Pt}(\text{thpy})_2$ with a significant MLCT admixture to the lowest ${}^3\text{LC}$ state, it is even reduced by six to seven orders of magnitude as compared to the organic emitters, and one finds a radiative decay time of the order of 1 μs (Fig. 8). For completeness, it is remarked that the values given refer to an average radiative decay of the triplet, since the different triplet substates exhibit distinctly different decay properties (e.g., see the following subsection and [79]).

In summary, for organometallic compounds the transition probability between the T_1 and the S_0 states can be tuned by several orders of magnitude as compared to organic emitters. This is mainly induced by an increase of spin-orbit coupling. Thus, the radiative processes can well compete with the non-radiative ones. Consequently, organo-transition-metal compounds can exhibit efficient emissions (phosphorescence) and therefore are well suited as emitter materials for OLEDs.

5.4 Zero-Field Splitting

Triplet states split generally into substates. This is also valid for purely organic molecules. However, for these one finds only small values of ZFS of the order of 0.1 cm^{-1} which result from spin-spin coupling between the electrons in the π and π^* orbitals, respectively (e.g., see [80–82]). On the other hand, in organo-transition-metal compounds SOC will modify the triplet states' properties by mixing in higher lying states of singlet and triplet character. Already small admixtures have drastic consequences. For example, one finds an increase of the ISC rate (see above) and of the phosphorescence decay rate (see previous subsection) by orders of magnitude, although the ZFS is not yet distinctly altered [79]. Well studied examples with this behavior are $[\text{Rh}(\text{bpy})_3]^{3+}$ and $\text{Pd}(\text{qol})_2$ (=Pdq₂) [81, 93, 94].

Higher metal participation and larger SOC lead to distinct ZFSs as has already been discussed and depicted in Fig. 7. Importantly, the individual triplet substates can have very different photophysical properties with regard to

radiative decay rates, vibronic coupling, coupling to the environment, emission quantum yields, population and relaxation dynamics due to spin-lattice relaxation, sensitivity with respect to symmetry changes, etc. [25, 34, 75–79, 81, 87, 89–91, 93–97]. At ambient temperature, the individual properties are largely smeared out and one finds mostly only an averaged behavior. Nevertheless, the individual triplet substates still determine the overall emission properties.

5.5

Emission Band Structure and Vibrational Satellites

At ambient temperature, the phosphorescence of organometallic compounds consists usually of superimposed spectra, which stem from the different triplet substates (see previous subsection, Fig. 8). An individual spectrum which results from one specific substate is composed of a transition at the electronic origin (0–0 transition), a large number of vibrational satellites, and of in part overlapping low-energy satellites which involve librations of the complex in its environment. Moreover, all of these individual transitions are smeared out by inhomogeneity effects. Thus, at ambient temperature normally only a broad-band emission results. Sometimes residual, moderately resolved structures occur, which often stem from overlapping vibrational satellites (not necessarily from progressions). Interestingly, at low temperature and under suitable conditions, these structures can be well resolved and characterized [34, 75–79, 89–91, 93–103]. From this kind of investigations it follows that the vibrational satellite structure is also influenced by metal participation in the electronic states [100]. Specifically, the spectra of compounds with electronic transitions of mainly LC($\pi\pi^*$) character (small metal participation) are largely determined by satellites corresponding to ligand vibrations (fundamentals, combinations, progressions). However, with increasing metal participation, low-energy vibrational satellites of metal-ligand character grow in additionally (up to about 600 cm^{-1} from the electronic origin) [100] (Fig. 8). Thus, the maximum of the unresolved emission spectrum shifts towards the electronic 0–0 transition.

To summarize, metal participation in the emitting state leads to a slight blue shift of the unresolved emission maximum as compared to an LC spectrum with the same 0–0 transition energy. Moreover, the occurrence of additional low-energy metal-ligand vibrational satellites causes a further smearing out of the spectrum. The slight spectral shift might be of interest for fine-tuning of the emission color.

5.6

Electronic Charge Distribution and Excited State Reorganization

The singlet-triplet transitions of compounds with small metal character, situated on the left hand side of Fig. 7, are localized to one of the ligands, even if the formal symmetry of the complex would allow a delocalization over all of the ligands. This has been proven for $[\text{Rh}(\text{bpy})_3]^{3+}$ [93] and $[\text{Pt}(\text{bpy})_2]^{2+}$ [101] by use of the method of deuteration labeling [76, 78]. On the other hand, for compounds with emissive $^3\text{MLCT}$ states such as $[\text{Ru}(\text{bpy})_3]^{2+}$ [102] and $[\text{Os}(\text{bpy})_3]^{2+}$ [103] it has been shown that the excited state is delocalized over the three ligands and the metal [76, 78, 102, 103]. This is even valid for $\text{Pt}(\text{thpy})_2$, in which the triplet state is largely of $\text{LC}(\pi\pi^*)$ character, but for which the metal orbital admixture induces sufficient coupling between the ligands (Fig. 7, middle). Thus, one obtains a delocalization in the lowest excited state [78, 79]. It is remarked that these results were determined for compounds doped into rigid matrices.

Moreover, since the metal character or MLCT contribution in the triplet state, if sufficiently large, can induce a ligand-ligand coupling that delocalizes the excited state wavefunction, the metal contribution will also affect the geometry change that follows an excitation. For the localized situation in the compounds mentioned above, one finds a maximum Huang-Rhys parameter [79] of $S=0.3$, while for the compounds with delocalized triplets, this characteristic parameter is by a factor of three to four smaller [76, 79]. Geometry changes or reorganization effects which occur upon excitation of the emissive triplet states are small for nearly all of the complexes investigated (in rigid matrices). However, it can be concluded that the reorganization effects are further minimized for those organometallic compounds with high metal participation in the triplet states (complexes at the right hand side of Fig. 7). The emissive states of these compounds exhibit a weaker coupling to the environment and therefore represent good candidates for OLED emitter materials with high emission quantum yields.

6

Summary and Conclusion

Organo-transition-metal triplet emitters have a great potential to be applied in OLEDs. Thus, an understanding of the processes, which lead to electron-hole recombination (exciton formation) and to the population of the emissive triplet states is presented. In particular, it is shown that the dynamical process of exciton formation and trapping on an emitter molecule involves charge transfer states which result from excitations of the dopant to its nearest neighbor matrix environment ($^{1,3}\text{DMCT}$ states). Individual singlet and triplet trapping and relaxation paths lead to the population of the lowest ex-

cited singlet and triplet states of the dopant. In typical organic molecules with weak spin-orbit coupling and highly forbidden triplet-singlet transitions, triplet state population is transferred into heat (at ambient temperature). Only the singlet can emit radiatively (fluorescence). On the other hand, in organo-transition-metal compounds, fast intersystem crossing induced by spin-orbit coupling effectively depopulates the excited singlet into the lowest triplet. Again, due to SOC, the triplet can decay radiatively as phosphorescence even with high emission quantum yield at ambient temperature. In case of validity of spin statistics only 25% of the excitons can be exploited by organic emitters, while for triplet emitters additional 75% of the excitons are harvested in the triplet states. Thus due to triplet harvesting, the efficiency of light emission in an electro-luminescent device with triplet emitters can be—in the limit of vanishing radiationless deactivation—higher by a factor of four compared with singlet emitters. Moreover, on the basis of a detailed knowledge about the photophysical properties of organo-transition-metal emitters, clear trends are elucidated for triplet emitters. This leads to the possibility to control important factors, such as metal participation and spin-orbit coupling in the triplet states, by chemical variation. Thus, the controlled development of compounds with predefined photophysical properties will be achievable. Specifically, increase of metal participation and SOC is displayed in a growing zero-field splitting of the triplet into substates. This parameter can be determined experimentally. The corresponding ZFS values of the compounds discussed in this investigation vary by more than a factor of 2000. In particular, increasing metal character lowers the energy of the excited singlet, reduces the energy separation between the excited singlet and triplet states, enhances the intersystem crossing rate from the lowest excited singlet to the lowest triplet, lowers the emission decay time by increasing the radiative rate between the triplet and the singlet ground state, changes the vibrational satellite structure and thus the spectral distribution of the emission band, decreases the excited state reorganization energy, etc. This promising new concept is not only applicable to small molecules, it can also usefully be applied if combined with other strategies, which are based, for example, on the use of functionalized ligands [104], dendrimeric shielding effects [14, 105], and attachments of organo-metallic compounds to polymers [106].

Acknowledgement Financial support of the Bundesministerium für Bildung und Forschung (BMBF) is acknowledged.

References

1. Hagfeldt A, Grätzel M (2000) *Acc Chem Res* 33:269
2. Kuciauskas D, Freund MS, Gray HB, Winkler JR, Lewis NS (2001) *J Phys Chem B* 105:392

3. Tai WP, Inoue K, Oh JH (2002) *Sol Energy Mater* 71:553
4. Demas JN, DeGraff BA (2001) *Coord Chem Rev* 211:317
5. Liebsch G, Klimant I, Frank B, Holst G, Wolfbeis OS (2000) *Appl Spectrosc* 54:548
6. Buss CE, Mann KR (2002) *J Am Chem Soc* 124:1031
7. Guo X-Q, Castellano FN, Li L, Szmecinski H, Lakowicz JR, Sipior J (1997) *Anal Chem* 63:337
8. Cary DR, Zaitseva NP, Gray K, O'Day KE, Darrow CB, Lane SM, Peyser TA, Satcher JH Jr, VanAntwerp WP, Nelson AJ, Reynolds JG (2002) *Inorg Chem* 41:1662
9. Drew SM, Janzen DE, Buss CE, MacEwan DI, Dublin KM, Mann KR (2001) *J Am Chem Soc* 123:8414
10. Wei L, Chan MCW, Cheung K-K, Che C-M (2001) *Organometallics* 20:2477
11. Lamansky S, Djurovich PI, Murphy D, Abdel-Razzaq F, Kwong R, Tsyba I, Bortz M, Mui B, Bau R, Thompson ME (2001) *Inorg Chem* 40:1704
12. Brooks J, Babayan Y, Lamansky S, Djurovich PI, Tsyba I, Bau R, Thompson ME (2002) *Inorg Chem* 41:3055
13. Grushin VV, Herron N, LeCloux DD, Marshall WJ, Petrov VA, Wang Y (2001) *Chem Commun* 1494
14. Lo S-C, Male NAH, Markham JPI, Magennis SW, Burn PL, Salata OV, Samuel IDW (2002) *Adv Mater* 14:975
15. Tsuzuki T, Shirasawa N, Suzuki T, Tokito S (2003) *Adv Mater* 15:1455
16. Nazeeruddin MK, Humphry-Baker R, Berner D, Rivier S, Zuppiroli L, Graetzel M (2003) *J Am Chem Soc* 125:8790
17. Juris A, Balzani V, Barigelletti F, Campagna S, Belser P, von Zelewsky A (1988) *Coord Chem Rev* 84:85
18. Caspar JV, Meyer TJ (1983) *Inorg Chem* 22:2444
19. Kober EM, Marshall JL, Dressick WJ, Sullivan BP, Caspar JV, Meyer TJ (1985) *Inorg Chem* 24:2755
20. Kober EM, Caspar JV, Lumpkin RS, Meyer TJ (1986) *J Phys Chem* 90:3722
21. Kinnunen T-JJ, Haukka M, Nousiainen M, Patrikka A, Pakkanen TA (2001) *J Chem Soc Dalton Trans* 2649
22. Kalyanasundaram K (1992) *Photochemistry of polypyridine and porphyrin complexes*. Academic Press, London
23. Caspar JV, Meyer TJ (1983) *J Phys Chem* 87:952
24. Striplin DR, Crosby GA (1994) *Chem Phys Lett* 221:426
25. Finkenzeller W, Stößel P, Kulikova M, Yersin H (2004) *Proc SPIE* 5214:356
26. Roundhill DM (1994) *Photochemistry and photophysics of metal complexes*. Plenum Press, New York
27. Vogler A, Kunkely H (2001) *Top Curr Chem* 213:143
28. Lai S-W, Che C-M (2004) *Top Curr Chem* 241:37
29. Maestri M, Balzani V, Deuschel-Cornioley C, von Zelewsky A (1992) *Adv Photochem* 17:1
30. Caspar JV, Sullivan BP, Kober EM, Meyer TJ (1982) *Chem Phys Lett* 91:91
31. Timpson CJ, Bignozzi CA, Sullivan BP, Kober EM, Meyer TJ (1996) *J Phys Chem* 100:2915
32. Chen P, Meyer TJ (1998) *Chem Rev* 98:1439
33. Sullivan BP (1989) *J Phys Chem* 93:24
34. Wiedenhofer H, Schützenmeier S, von Zelewsky A, Yersin H (1995) *J Phys Chem* 99:13385
35. Auzel F (1980) In: DiBartolo B (ed) *Radiationless processes*. Plenum Press, New York

36. Mataga N, Kubota T (1970) *Molecular interactions and electronic spectra*. Marcel Dekker, New York
37. DiBartolo B (ed) (1980) *Radiationless processes*. Plenum Press, New York
38. Turro NJ (1978) *Modern molecular photochemistry*. Benjamin/Cummings Publ, Menlo Park, California, USA
39. Flint CD (ed) (1989) *Vibronic processes in inorganic chemistry*. Kluwer Academic Publishers, Dordrecht, Series C, Mathematical and Physical Sciences, vol 288
40. Fukase A, Dao KLT, Kido J (2002) *Polym Adv Technol* 13:601
41. Zhou X, Qin DS, Pfeiffer M, Blochwitz-Nimoth J, Werner A, Drechsel J, Maennig B, Leo K, Bold M, Erk P, Hartmann H (2002) *Appl Phys Lett* 81:4070
42. Adachi C, Baldo MA, Forrest SR, Lamansky S, Thompson ME, Kwong RC (2001) *Appl Phys Lett* 78:1622
43. Kawamura Y, Yanagida S, Forrest SR (2002) *J Appl Phys* 92:87
44. Baldo MA, Lamansky S, Burrows PE, Thompson ME, Forrest SR (1999) *Appl Phys Lett* 75:4
45. Fuhrmann T, Salbeck J (2002) *Adv Photochem* 27:83
46. Lee C-L, Lee KB, Kim J-J (2000) *Appl Phys Lett* 77:2280
47. Nguyen TP, LeRendu P, Dinh NN, Fourmigue M, Mézière C (2003) *Synth Met* 138:229
48. Wang X, Rundl P, Bale M, Mosley A (2003) *Synth Met* 137:1051
49. Riel H, Karg S, Beierlein T, Ruhstaller B, Riefl W (2003) *Appl Phys Lett* 82:466
50. Lee Y-J, Kim S-H, Huh J, Kim G-H, Lee Y-H, Cho S-H, Kim Y-C, Do YR (2003) *Appl Phys Lett* 82:3779
51. Pfeiffer M, Forrest SR, Leo K, Thompson ME (2002) *Adv Mater* 14:1633
52. Murata H, Kafafi ZH, Uchida M (2002) *Appl Phys Lett* 80:189
53. Liu MS, Luo J, Jen AK-Y (2003) *Chem Mater* 15:3496
54. Chen HY, Lam WY, Luo JD, Ho YL, Tang BZ, Zhu DB, Wong M, Kwok HS (2002) *Appl Phys Lett* 81:574
55. Watkins NJ, Mäkinen AJ, Gao Y, Ushida M, Kafafi ZH (2004) *Proc SPIE* 5214:368
56. Tung Y-J, Lu MM-H, Weaver MS, Hack M, Brown JJ (2004) *Proc SPIE* 5214:114
57. Chwang AB et al. (2003) *Appl Phys Lett* 83:413
58. Huang W, Wang X, Sheng M, Xu L, Stubhan F, Luo L, Feng T, Wang X, Zhang F, Zou S (2003) *Mater Sci Eng B* 98:248
59. Müller CD, Falcon A, Reckefuss N, Rojahn M, Wiederhirn V, Rudati P, Frohne H, Nuyken O, Becker H, Meerholz K (2003) *Nature* 421:829
60. Kim C, Forrest SR (2003) *Adv Mater* 15:541
61. Auch MDJ, Soo OK, Ewald G, Soo-Jin C (2002) *Thin Solid Film* 417:47
62. Gong X, Robinson MR, Ostrowski JC, Moses D, Bazan GC, Heeger AJ (2002) *Adv Mater* 14:581
63. O'Brien DF, Giebeler C, Fletcher RB, Cadby AJ, Palilis LC, Lidzey DG, Lane PA, Bradley DDC, Blau W (2001) *Synth Met* 116:379
64. Tutiš E, Berner D, Zuppiroli L (2003) *J Appl Phys* 93:4596
65. Lamansky S, Kwong RC, Nugent M, Djurovich PI, Thompson ME (2001) *Org Electron* 2:53
66. Hellwege K-H (1976) *Einführung in die Festkörperphysik*. Springer, Berlin Heidelberg New York, p 509
67. Garten F, Hilberer A, Cacially C, Esselink E, vanDam Y, Schlachtmann B, Friend RH, Klapwijk TM, Hadziioannou (1997) *Adv Mater* 9:127
68. Burin AL, Ratner MA (1998) *J Chem Phys* 109:6092
69. Shuai Z, Beljonne D, Silbey RJ, Brédas JL (2000) *Phys Rev Lett* 84:131
70. Hong T-M, Meng H-F (2001) *Phys Rev B* 63:075206

71. Wohlgenannt M, Tandon K, Mazumdar S, Ramasesha S, Vardeny ZV (2001) *Nature* 409:494
72. Virgili T, Cerullo G, Lüer L, Lanzani G, Gadermaier C, Bradley DDC (2003) *Phys Rev Lett* 90:247402
73. Baldo MA, O'Brien DF, You Y, Shoustikov A, Silbley S, Thompson ME, Forrest SR (1998) *Nature* 395:151
74. Cleave V, Yahioglu G, LeBarny P, Friend RH, Tessler N (1999) *Adv Mater* 11:285
75. Yersin H, Humbs W, Strasser J (1997) *Coord Chem Rev* 159:325
76. Yersin H, Humbs W, Strasser J (1997) *Top Curr Chem* 191:153
77. Yersin H, Strasser J (1997) *J Lumin* 72/74:462
78. Yersin H, Humbs W (1999) *Inorg Chem* 38:5820
79. Yersin H, Donges D (2001) *Top Curr Chem* 214:81
80. Lumb MD (ed) (1978) *Luminescence spectroscopy*. Academic Press, London
81. Glasbeek M (2001) *Top Curr Chem* 213:95
82. Azumi T, Miki H (1997) *Top Curr Chem* 191:1
83. Komada Y, Yamauchi S, Hirota N (1986) *J Phys Chem* 90:6425
84. Ikeda S, Yamamoto S, Nozaki K, Ikeyama T, Azumi T, Burt JA, Crosby GA (1991) *J Phys Chem* 95:8538
85. Colombo MG, Hauser A, Güdel HU (1994) *Top Curr Chem* 171:143
86. Funayama T, Kato M, Kosugi H, Yagi M, Higuchi J, Yamauchi S (2000) *Bull Chem Soc Jpn* 73:1541
87. Finkenzeller WJ, Yersin H (2003) *Chem Phys Lett* 377:299
88. Hay PJ (2002) *J Phys Chem A* 106:1634
89. Yersin H, Schützenmeier S, Wiedenhofer H, von Zelewsky A (1993) *J Phys Chem* 97:13496
90. Schmidt J, Wiedenhofer H, von Zelewsky A, Yersin H (1995) *J Phys Chem* 99:226
91. Glasbeek M, Sitters R, van Veldhofen E, von Zelewsky A, Humbs W, Yersin H (1998) *Inorg Chem* 37:5159
92. Pierloot K, Ceulemans A, Merchán M, Serrano-Andrés L (2000) *J Phys Chem A* 104:4374
93. Humbs W, Yersin H (1996) *Inorg Chem* 35:2220
94. Yersin H, Donges D, Nagle JK, Sitters R, Glasbeek M (2000) *Inorg Chem* 39:770
95. Yersin H, Strasser J (2000) *Coord Chem Rev* 208:331
96. Strasser J, Homeier HHH, Yersin H (2000) *Chem Phys* 255:301
97. Yersin H, Donges D, Humbs W, Strasser J, Sitters R, Glasbeek M (2002) *Inorg Chem* 41:4915
98. Yersin H, Kratzer C (2002) *Coord Chem Rev* 229:75
99. Yersin H, Kratzer C (2002) *Chem Phys Lett* 362:365
100. Yersin H, Huber P, Wiedenhofer H (1994) *Coord Chem Rev* 132:35
101. Humbs W, Yersin H (1997) *Inorg Chim Acta* 265:139
102. Braun D, Huber P, Wudy J, Schmidt J, Yersin H (1994) *J Phys Chem* 98:8044
103. Huber P, Yersin H (1993) *J Phys Chem* 97:12705
104. Chan WK, Ng PK, Gong X, Hou S (1999) *Appl Phys Lett* 75:3920
105. Furata P, Brooks J, Thompson ME, Fréchet MJM (2003) *J Am Chem Soc* 125:13165
106. Chen X, Liao J-L, Liang Y, Ahmed MO, Tseng H-E, Chen S-A (2003) *J Am Chem Soc* 125:636